Development of a New Recoil Filter Detector for γ-Detector Arrays

J. Heese, K.H. Maier, H. Grawe, H. Kluge, M. Schramm, R. Schubart, K. Spohr
Hahn-Meitner-Institut GmbH, Berlin, Germany

W. Meczynski, M. Janicki, J. Styczen, J. Grebosz
Henryk Niewodniczanski Institute of Nuclear Physics, Cracow, Poland

A new device for the detection of evaporation residues in coincidence with γ rays in heavy-ion induced reactions is presented. This new detector mainly discriminates against fission and allows Doppler corrections of the γ spectra. As a first application, the level schemes of the neutron deficient lead isotopes ^{188}Pb and ^{186}Pb have been studied for the first time at the VICKSI accelerator. Both nuclei exhibit a structure different from heavier even-even Pb isotopes and show low-lying rotational bands.

I. Introduction

The operation of large arrays of Compton suppressed HP Germanium detectors in coincidence with electromagnetic recoil mass separators (RMS) has allowed the investigation of many nuclei near the proton dripline and therefore yielded information about the shell structure which stabilizes nuclei [1-3]. The observation of nuclei populated in heavy-ion induced fusion-evaporation reactions with only 10^{-3} of the total cross section was possible because the γ ray spectra were filtered with the Z and A information of the evaporation residue. However, the price for this unique exit channel selection is the low efficiency of the existing recoil mass separators. A considerable improvement of γ spectra can still be achieved when evaporation residues are detected in coincidence with γ rays, even without Z and A information. This coincidence suppresses γ rays from competing fission or transfer processes, Coulomb excitation and reactions with target contaminations and therefore cleans γ spectra and improves the peak/background ratio. In addition, the determination of the velocity vector of the evaporation residue allows Doppler corrections and therefore a gain in energy resolution. With this in mind, a sturdy time-of-flight filter for evaporation residues has been designed as an additional detector for the OSIRIS spectrometer consisting of 12 Compton suppressed Germanium detectors and a 48 element BGO γ multiplicity filter [4]. The main application of this new detector is to suppress γ rays from fission products as the dominant source of background for the in-beam spectroscopy of neutron deficient nuclei in the lead or actinide region.

II. Detector Development

A schematic diagram of the OSIRIS setup with recoil filter detector RFD is shown in the upper part of figure 1. The RFD consists of two rings of 6 and 12 individual detector elements mounted 73cm from the target under forward angles between 2.7° and 12.1° to the beam axis. At this distance, heavy evaporation residues (ER) produced with not too heavy beams are well-separated in time of flight from all other reaction products. Since the RFD requires only a narrow forward cone (200 mrad), it can be used with all 48 elements of the BGO ball, only the most forward Ge detector had to be removed for mechanical reasons.

In each RFD element, nuclei hitting a 2μm thick aluminised Mylar foil produce n secondary electrons which are electrostatically accelerated up to 20 keV and focussed onto a thin (5 to 10μm) plastic scintillator in which they produce a signal of n$\times$20keV. The geometry of the electron lens is shown in figure 1b. Electron yields of n$\approx$200/ion are expected from slow and heavy evaporation residues [5]. Since the heavy ion-induced secondary electron yields are proportional to the electronic energy loss of the projectile [5,6], recoiling evaporation residues can be discriminated from scattered beam not only via the time-of-flight separation but also from the pulse height of the scintillator signal. This signal is fast enough (20ns double pulse resolution) to allow the detection of evaporation residues even if scattered beam hits the detector before. During experiment, 1-2% of the initial beam is scattered into the inner RFD ring causing high countrates. Therefore, signals from scattered beam are suppressed by selecting only RFD signals in a time window appropriate for evaporation residues relative to the pulsed beam. In a second stage a γ-γ-RFD coincidence is required. Parameters measured are the time-of-flight with respect to the radio frequency of

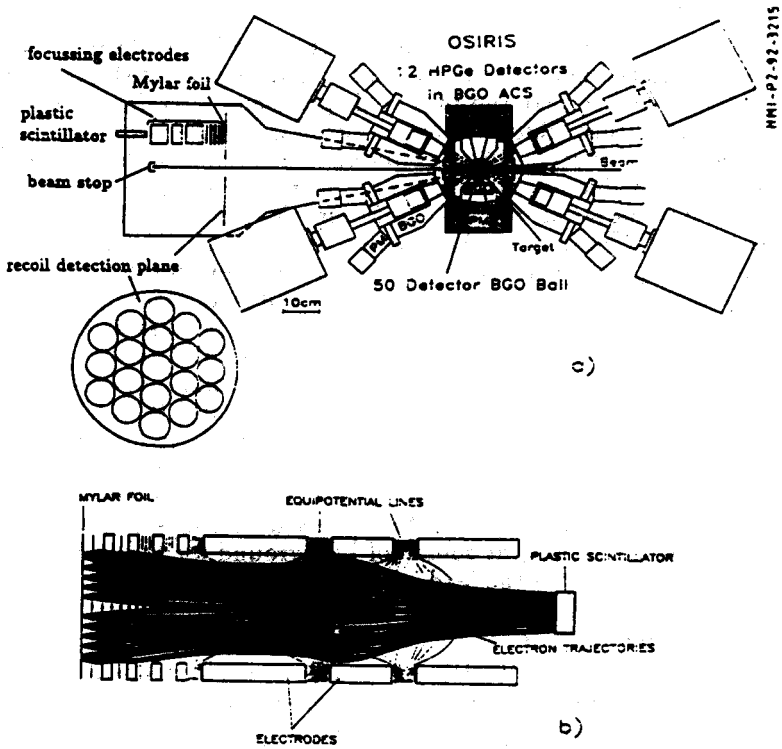

Figure 1: Schematic view of OSIRIS plus RFD. The 18 detection elements are arranged in the detection plane on concentric rings as shown in (a), the central hole holds the beam stop. For reasons of clarity only one detector element is drawn which is magnified in (b).

the VICKSI cyclotron and the responding detector element that determines the recoil angle. Velocity and angle of the nuclei are measured well enough to correct the Doppler shift of the γ-rays to a much better accuracy than the resolution of Ge detectors.

The RFD detection efficiency depends on the geometrical efficiency and on the fraction of recoils scattered into the sensitive angular range of the device and thus on reaction parameters and target thickness. The amount of beam and evaporation residues scattering into the active RFD area (2.7° to 12.1°) can be calculated using Monte-Carlo-simulations of ion-beam interactions with solids, e.g. the program TRIM [7]. If one only considers (HI,xn) reactions with ER masses m≈200 where the momentum transfer of the evaporated particles is small, the multiple scattering in the target is the dominant factor that determines the opening angle of the recoil cone and thus the RFD efficiency. In the reaction ^{124}Sn(^{40}Ar,5n)^{159}Er at 185 MeV, efficiencies between 20 % and 50 % can be expected from TRIM calculations for target thicknesses between 0.5 and 1.4 mg/cm^2.

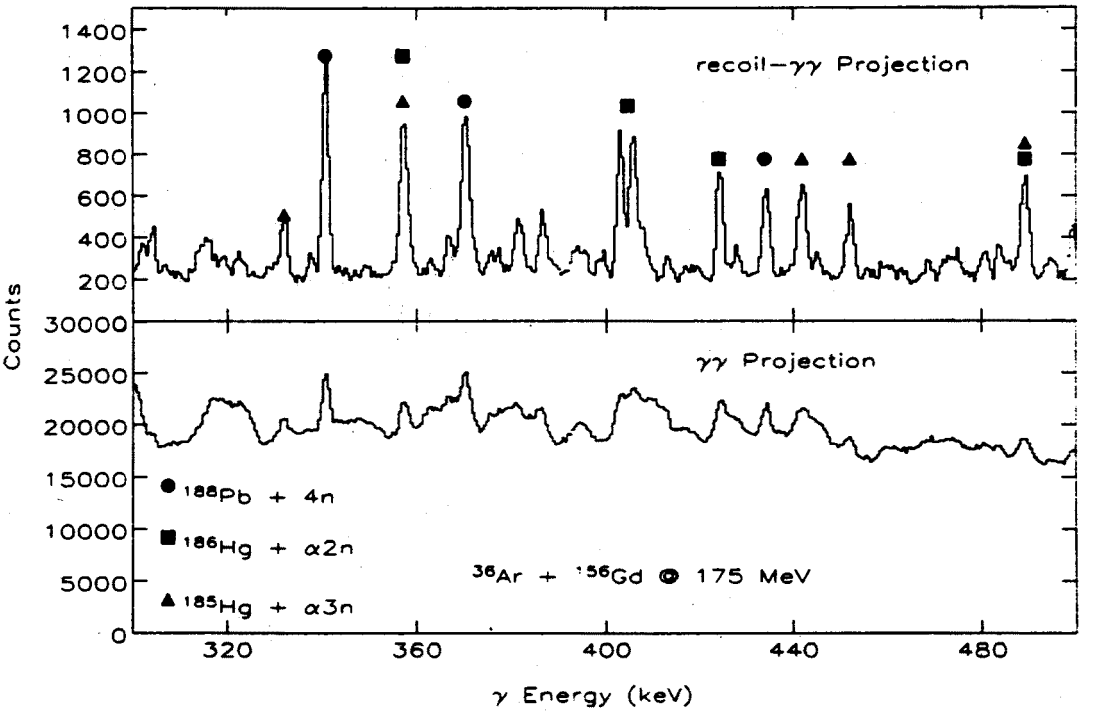

Figure 2: Comparison of a $\gamma\gamma$ projection with a recoil gated $\gamma\gamma$ projection. For details see text.

First in-beam test experiments with only four Compton suppressed Ge detectors and RFD were performed with the reactions $^{40}Ar + ^{124}Sn$ and $^{40}Ar + ^{152}Sm$ at 185 MeV. In these runs, γ single spectra and recoil gated γ spectra were recorded. The recoil detection efficiency determined from (recoil-γ)/γ intensity ratios was 31% in the first run (using a 1.4 mg/cm^2 target) and 18% in the second run (with a 0.7 mg/cm^2 target). First experiments using the full OSIRIS array plus RFD aimed at the spectroscopic investigation of the lead isotopes $^{186,188}Pb$. The reactions $^{154,156}Gd(^{36}Ar,4n)^{186,188}Pb$ at 175 MeV were used with 1.2 mg/cm^2 targets, yielding a RFD efficiency of 12%. In all experiments only about half of the efficiency expected from TRIM calculations was achieved. This is most likely due to a loss of electron transmission in the RFD elements when nuclei hit the outer sections of the Mylar foil.

Figure 2 shows a $\gamma\gamma$-projection from the ^{188}Pb run compared to the corresponding recoil-$\gamma\gamma$ projection. The $\gamma\gamma$- data were gated with a BGO ball multiplicity $m_\gamma \geq 3$, already eliminating much background, and corrected for Doppler broadening using the average recoil velocity and Ge detector angles measured with respect to the beam axis. The recoil-$\gamma\gamma$ data were Doppler-corrected event-by-event using the measured recoil velocity and angles between Ge detector and RFD element. The background in the recoil-$\gamma\gamma$ spectra is reduced by a factor of 85 compared to $\gamma\gamma$ data. The effect of Doppler corrections is most pronounced for α evaporation channels. It can be seen from figure 2 that despite the low detection efficiency of only 12% the requirement of recoil-$\gamma\gamma$ coincidences effectively cleans the spectra from unwanted background and improves the energy resolution.

III. Spectroscopy of ^{188}Pb and ^{186}Pb

Transitions in the previously unknown isotopes ^{188}Pb and ^{186}Pb were identified by γ-X-ray coincidences. Figure 3 shows a sum of coincidence spectra of the observed ^{188}Pb lines, the inset shows the level scheme established from recoil-$\gamma\gamma$ coincidences. The $2^+ \rightarrow 0^+$ assignment of the 724 keV state is suggested for two reasons: (i) the line at 724 keV is the most intense one and (ii) a 2^+ energy of about 730 keV in ^{188}Pb is expected from systematics.[8] All other lines were placed in the level scheme according to their intensities. Assuming that the line at 724 keV is the ^{188}Pb ground state transition, measured DCO ratios (table 1) indicate a stretched E2 nature of all transitions shown in figure 3. The transitions 370, 434, 499, 558, 606 and 634 keV thus seem to form a rotational band starting with fairly constant energy spacings of $\Delta E_\gamma = 65$ keV.

In a second experiment, a search for delayed γ-rays in ^{188}Pb was carried out. ^{188}Pb was populated again via $^{156}Gd(^{36}Ar,4n)$ at 175 MeV using a 10 mg/cm^2 target on a 50 mg/cm^2 gold backing. The separation between the VICKSI beam pulses was 330 ns. In this experiment, the level scheme shown in figure 3 could be confirmed and three new transitions were found. These transitions are delayed and were observed in a time window from 40 to 300 ns after the prompt γ time peak. However, lifetimes of the new levels could not be measured due to the weak intensity of the transitions. The ^{188}Pb level scheme deduced from both experiments is shown in figure 4, a summary of the measured γ energies, intensities and DCO ratios is given in table 1. Arguing from systematics of spherical 4^+ states in $^{190-198}Pb$, the 472 keV transition feeding the 724 keV state is most likely due to the decay of the spherical 4^+ state in ^{188}Pb

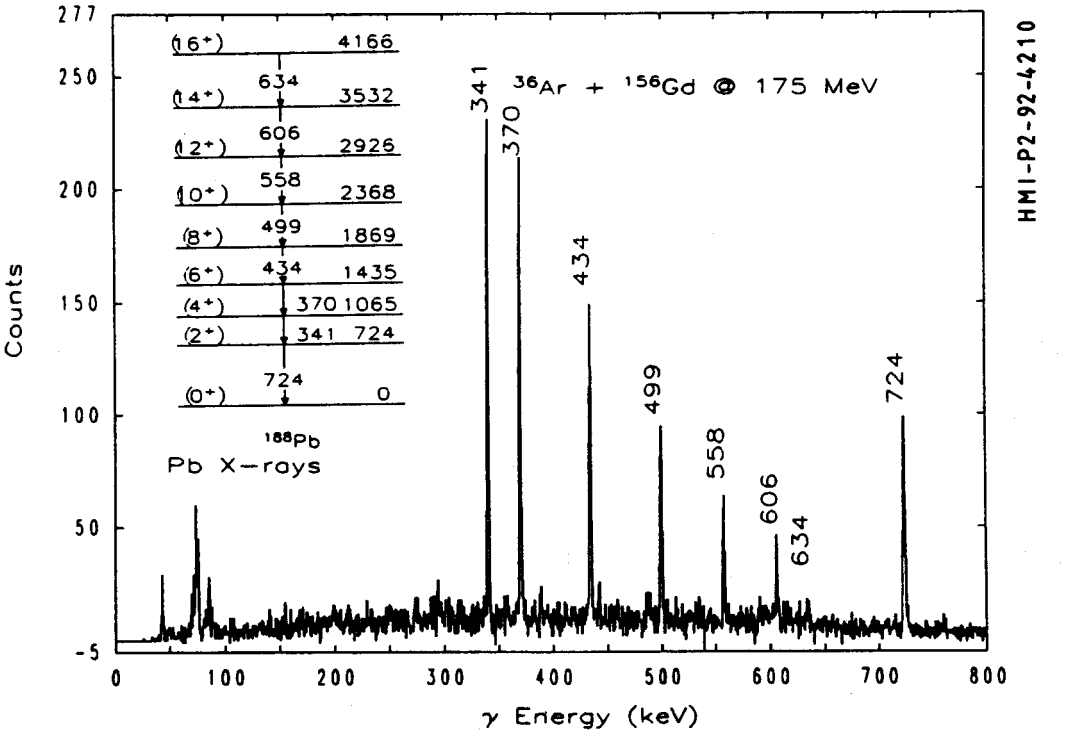

Figure 3: Summed coincidence spectrum of the labeled transitions in ^{188}Pb from recoil-$\gamma\gamma$ data. The inset shows the level scheme deduced from these data.

which is no longer yrast. The transitions of 336 and 345 keV both feed into the rotational state at 2.368 keV. A tentative spin-parity $I^{\pi} = (9^-)$ and (11^-) of the levels at 2.7 MeV excitation energy is suggested from the systematics of 9^- and 11^- states in the heavier Pb isotopes.

Figure 5 shows a spectrum of coincident γ rays assigned to ^{186}Pb from recoil-$\gamma\gamma$ coincidences recorded in the ^{36}Ar + ^{154}Gd run. Again, the identification was supported by X-ray-γ coincidences. A tentative level scheme of ^{186}Pb is shown in the inset of figure 5. Again, the transitions 261, 337, 413 and 486 keV seem to form a rotational band starting with constant energy spacings of ΔE_{γ}=75 keV. However, due to the weak intensities, DCO ratios could not be measured in this case and the spin-parity assignments are only suggested from the similarities with ^{188}Pb. In this experiment, the detection of the designated ^{186}Pb ground state transition at 662 keV would not have been possible without recoil-$\gamma\gamma$ coincidences.

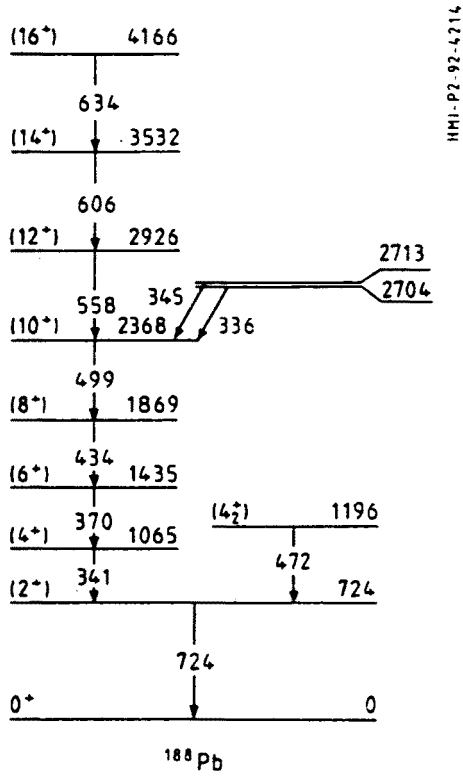

Figure 4: Deduced level scheme of ^{188}Pb.

IV. Discussion

The occurence of low-lying 0_2^+ states in neutron deficient lead isotopes is known [8,9] and ascribed to a shallow oblate minimum in the potential energy surface (PES) of these nuclei arising from the excitation of two-quasiparticle $h_{9/2}^2 s_{1/2}^{-2}$ proton intruder states. Although the 0_2^+ levels are the first excited states in $^{190-194}$Pb, these states or rotational bands built on these states have never been observed in heavy-ion induced reactions. It was shown by Van Duppen et al. [9] that the 0_2^+ energies in $^{196-190}$Pb can be calculated quite well from the positions of the (1qp) $\pi h_{9/2}[505]9/2^-$ and $\pi s_{1/2}[400]1/2^+$ bandheads in the neighbouring odd-A Tl and Bi isotopes using the equation

$$E_x(0_2^+,{}^A\mathrm{Pb}) = E_x(9/2^-,{}^{A-1}\mathrm{Tl}) + E_x(1/2^+,{}^{A+1}\mathrm{Bi}) + \Delta_c. \qquad (1)$$

Table 2 shows a comparison between experimental and calculated 0_2^+ energies in $^{188-196}$Pb. The experimental 0_2^+ energies in ^{188,186}Pb have been extrapolated from the rotational bands assuming a constant moment of inertia. The calculated values give a minimum of the 0_2^+ energy in ^{188}Pb, but the experimental results show a continuing drop of the measured 2^+ and extrapolated 0_2^+ energies in ^{186}Pb where the measured 2^+ energy is even lower than the calculated 0_2^+ energy. Thus, the bands in ^{188,186}Pb do not seem to follow these systematics and might have a different structure.

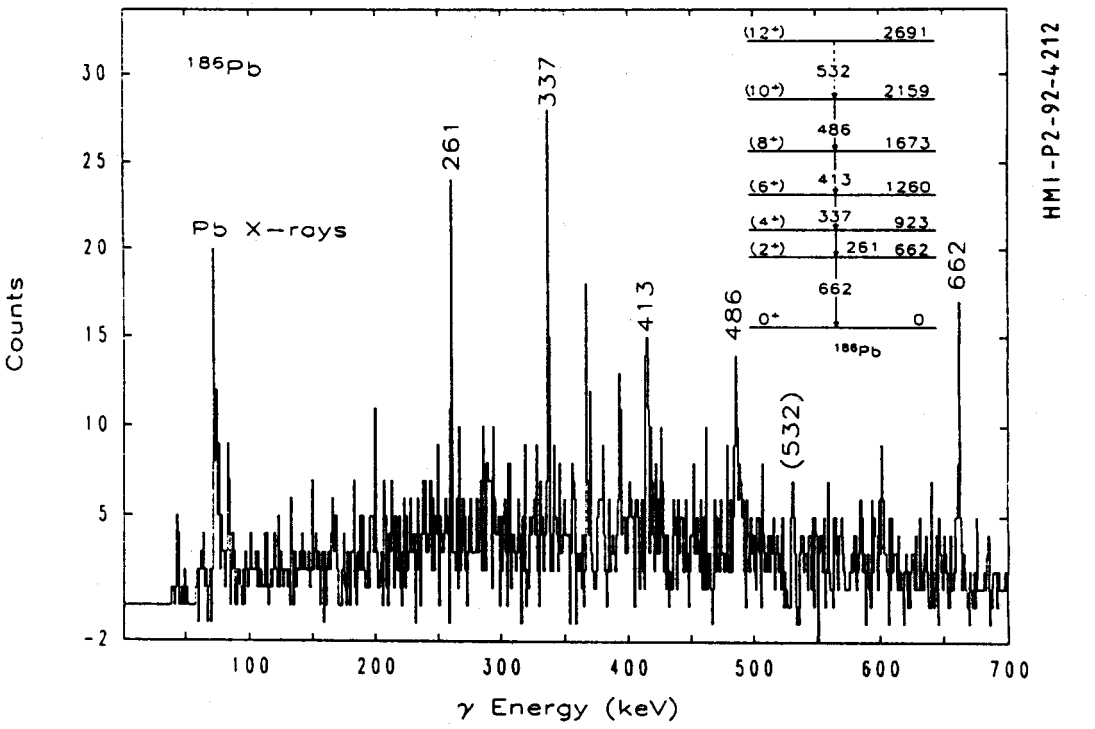

Figure 5: Summed coincidence spectrum of ^{186}Pb from recoil-$\gamma\gamma$ coincidences. The inset shows the tentative level scheme deduced from the observed coincidences.

Calculations using the Strutinsky shell correction method with a Woods-Saxon potential and a monopole pairing interaction have predicted well developed prolate minima of the potential energy surface in all Pb isotopes with N≤108 [10] which are ascribed to a $(\pi h_{9/2}[541]1/2^+)^2(s_{1/2}[400]1/2^+)^{-2}$ structure. The lowest predicted excitation energy of the prolate second minimum is 1.5 MeV in ^{186}Pb with a calculated deformation parameter $\beta_2 = 0.26$. Experimentally, the lowest rotational levels in ^{186,188}Pb are found around 1 MeV. Rotational structures very similar to these observed in ^{186,188}Pb are known in the isotones ^{184,186}Hg [12,13]. The rotational properties of these bands are in agreement with a prolate shape with $\beta_2 \approx 0.26$ and a rotational structure determined by $\nu i_{13/2}$, $\pi h_{9/2}$ and $\pi i_{13/2}$ quasiparticle excitations. Similar to the lead isotones, the energies of the rotational levels in ^{184}Hg decrease compared to ^{186}Hg while the energy spacings ΔE_γ of the lowest observed transitions increase. Thus, the rotational bands in ^{188,186}Pb might be the first experimental evidence for a prolate PES minimum in neutron deficient lead isotopes. The decrease in ΔE_γ in the ^{186,188}Pb bands at higher spins associated with a rise of the dynamic moments of inertia can then be attributed to a band crossing due to the rotational alignment of a $\nu i_{13/2}$ pair.

Table 1: Measured γ energies, intensities and DCO ratios in ^{188}Pb. The DCO ratios are defined in the following way:

$$R_{DCO} = \frac{Y(\gamma_1 \text{ at } 0° \text{ with gate on } \gamma_2 \text{ at } 90°)}{Y(\gamma_1 \text{ at } 90° \text{ with gate on } \gamma_2 \text{ at } 0°)}.$$

E_γ	I_γ^a	I_γ^b	R_{DCO}
723.9	100	100	0.96(7)[c]
340.8	91	82	0.96(7)[d]
370.3	92	80	1.06(10)[d]
434.4	75	43	1.07(9)[c]
499.4	60	35	1.10(11)[c]
557.7	35	17	1.22(16)[c]
606.1	22		1.07(20)[c]
634	9		
336.2		10[e]	
344.3		6[e]	
472.2		20[e]	

[a] γ intensities from the thin target run.
[b] γ intensities from the backed target run measured with the OSIRIS detectors centered around 0° and 180° and within a 300 ns time window.
[c] DCO ratio measured in coincidence with the 341 keV transition.
[d] DCO ratio measured in coincidence with the 724 keV transition.
[e] delayed γ transitions only observed in the backed target run.

Table 2: Calculated 0_2^+ energies in $^{186-196}$Pb. The $9/2^-$ and $1/2^+$ energies in the Tl and Bi isotopes were taken from [11].

	$E(0_2^+)_{exp}$	$E(9/2^-, {}^{A-1}Tl)$	$E(1/2^+, {}^{A+1}Bi)$	$E(0_2^+)$ [b]
^{196}Pb	1143	483	500	1143
^{194}Pb	926	365	401	930
^{192}Pb	766	299	307	769
^{190}Pb	683	281	242	658
^{188}Pb	520[a]	335	92	587
^{186}Pb	477[a]	454	60	674

[a] extrapolated from rotational levels.
[b] calculated from (1) with Δ_c=160(8)keV [9].

V. Summary

A new detection technique was developed for the in-beam spectroscopy of nuclei in heavy-ion induced reactions. The measurement of recoil-$\gamma\gamma$ coincidences was shown to be an effective filter against γ rays from fission processes. Thus, a RFD is a helpful additional detector for Germanium detector arrays with respect to background suppression and exit channel selection. This is particularly true for the spectroscopy of heavier nuclei where fission dominates. Although the measured efficiencies are still somewhat low compared to expected values, first experimental results obtained with the RFD look very promising. We have observed yrast states in the isotopes ^{186,188}Pb for the first time. Unlike the heavier even-even lead isotopes, these nuclei exhibit low-lying rotational bands very similar to their isotones ^{184,186}Hg. This highlights the influence of deformation-driving neutron levels when approaching the middle of the neutron shell.

This work was partially supported by the Polish state comittee for scientific research (KBN grant no. 204519101) and through the agreement on scientific cooperation between Poland and Germany.

References

[1] C.J. Lister et al., Phys. Rev. C 42, R1191 (1990).
[2] C.J. Gross et al., Phys. Rev. C 44, R2253 (1991).
[3] P.J. Ennis et al., Nucl. Phys. A 535, 392 (1991).
[4] R.M. Lieder et al., Nucl. Instr. Meth. A 220, 363 (1984).
[5] H.G. Clerc et al., Nucl. Instr. Meth. 113, 325 (1973).
[6] H. Rothard et al., in 'Particle Indudced Electron Emission II', Springer Tracts in Modern Physics, Vol. 123, Springer 1991.
[7] J.P. Biersack, L.G. Haggmark, Nucl. Instr. Meth. 174, 257 (1980).
[8] P. Van Duppen et al., Phys. Rev. Lett. 52, 1974 (1984) and Phys. Lett. B 154, 354 (1985).
[9] P. Van Duppen et al., Phys. Rev. C 35, 1861 (1987).
[10] R. Bengtsson and W. Nazarewicz, Z. Phys. A 334, 269 (1989).
[11] E. Coenen et al., Phys. Rev. Lett. 54, 1783 (1985).
[12] W.C. Ma et al., Phys. Lett. B 167, 277 (1986).
[13] R.V.F. Janssens et al., Phys. Lett. B 131, 35 (1983).